Optimization of Magnetic Relaxation and Isotopic Enrichment in Dimeric DyIII Single-Molecule Magnets

G. Huang, X. Yi, Julien Jung, O. Guillou, O. Cador, Fabrice Pointillart, Boris Le Guennic, Kevin Bernot

10.1002/ejic.201700842

FULL PAPER

Optimization of magnetic relaxation and isotopic enrichment in dimeric Dy^{III} single-molecule magnets

Gang Huang,[a] Xiaohui Yi,[a] Julie Jung,[b],[c] Olivier Guillou,[a] Olivier Cador,[b] Fabrice Pointillart,[b] Boris Le Guennic[b] and Kevin Bernot*[a]

Abstract: Single-molecule magnet (SMM) behavior on Dy-based dimers has been optimized by substitution of Dy^{III} ancillary ligand ($hfac^-$ in previously reported **DyPyNO**, for tta^- in **Dy**). Clear hysteresis opening is visible at 0.5K on **Dy** that allows for the determination of an antiferromagnetic coupling of -2.92 cm^{-1} (S=1/2, g_z=19.58) that is confirmed by *ab-initio* calculations. Comparison with **DyPyNO** shows that the strongest the AF coupling is, the better is the SMM behavior. This is further demonstrated by diamagnetic substitution and Y-Dy species (**YDy**) highlights that the strong AF magnetic interaction in **Dy** severely enhance magnetic relaxation at low T. This coupling is also expected to be at the origin of the unexpectedly weak isotopic effect observed on isotopically-pure parent of **Dy**, namely **161Dy** and **164Dy**.

Introduction

For the last twenty years, investigation of the magnetic behavior of isolated molecules has stimulated both chemists and physicists communities.[1] Molecular magnetism[2] has become an intense field of research and temperatures at which magnetic slow relaxation is observed have constantly been raised[3-6] especially when lanthanide ions have been used as paramagnetic centers.[7-10] Consequently, a flourishing of reports concerning lanthanide-based Single-Molecule Magnets (SMMs) has been observed.[11-13]

As far as magnetic slow relaxation is concerned, numerous works highlight the strong sensitivity of trivalent lanthanide ions to their electrostatic surrounding.[14-25] Oblate or prolate distribution of electronic density has been demonstrated to be a key ingredient in the realization of 4f-based SMM. This contradicts the general assumption that the shielding of the 4f orbitals of the lanthanides makes them non-sensitive to change in their neighboring. Minute changes in their coordination sphere, such as the position of second-sphere's hydrogen atoms,[26-28] drastically impact the orientation of their magnetic axis and their capabilities to behave or not as SMMs. Moreover the straightforward prolate/oblate theory[29] about lanthanide electronic surrounding and consequent ground-state stabilization is largely debated especially for Er^{III}[30,31] or Dy^{III}-based SMMs.[32] The picture is even more complex when magnetic couplings are observed.[25] As a consequence, lanthanide-based dimers[33-60] have been widely explored because they offer the most simple platform to investigate the magnetic couplings in lanthanide-based SMMs, that are expected to be some interplay between electrostatic[61] and exchange contributions.[50]

Recently, some of us reported a dimer of formula $[Dy(hfac)_3(NOPy)]_2$ (hfac= hexafluoroacetylacetonate, NOPy= pyridine *N*-oxide; compound latter called **DyPyNO**) that presents significant SMM properties (Δ= 167 K, τ= 5.62 10^{-11} s, α_{2K}= 0.05) and a Dy^{III}–Dy^{III} antiferromagnetic interaction (J_{exp}=-2.46 cm^{-1}, $g_{z\,exp}$= 18.69).[55] This dimer has been extensively investigated and sublimation of bulk powder can form either crystalline thick films[55] or amorphous thin films (≤200nm) with preserved magnetic properties.[62] Such dimers are then a nice playground to evaluate the effect of electronic change around the Dy^{III} ion by modifying either the bridging ligand (pyridine *N*-oxide moiety) or the ancillary ligands (β-diketonate moieties). We have investigated the first case recently and shown that substitution of bridging ligand by a NO_2 group allows enhancing the SMM properties of the dimers, a feature that is preserved also in thick films.[63] In this study we have chosen to investigate the influence of the ancillary ligand on dimer's properties by changing the $hfac^-$ ligand for tta^- ligand (tta^-= 2-thenoyltrifluoroacetonate).

Additionally, some of us recently demonstrated that metal-centered isotopic substitution is an efficient tool to optimize SMM properties.[64,65] The reduction of hyperfine coupling-driven quantum tunneling with nuclear spin-free ions ($^{164}Dy^{III}$) induces a spectacular optimization of the relaxation time in zero-field. We have thus used not only $Dy(tta)_3{\cdot}2H_2O$ precursors but also $^{161}Dy(tta)_3{\cdot}2H_2O$ and $^{164}Dy(tta)_3{\cdot}2H_2O$ precursors in this study to probe the isotopic effect on dimer's properties.

Results and Discussion

Crystal structure

Reaction of the aforementioned Dy adducts with NOpy ligand affords the three derivatives of formula $[Dy(tta)_3(NOPy)]_2$ latter called **161Dy**, **Dy** (for the natural derivative) and **164Dy**. Crystal structure has been solved on **Dy** and isostructurality with the other two derivatives is demonstrated on the basis of their powder X-ray diffraction patterns (Figure S1).

Dy crystallizes in the triclinic crystal system, P-1 space group. The asymmetric unit is made of one $Dy(tta)_3$ moiety and

[a] G.H., X.Y., O.G., K.B.,
Institut des Sciences Chimiques de Rennes (ISCR)
INSA-Rennes, 20 avenue des buttes de coësmes, 35708 Rennes, France.
kevin.bernot@insa-rennes.fr
[b] J.J., O.C., F.P., B. LG.,
Institut des Sciences Chimiques de Rennes (ISCR)
Université de Rennes 1, 263, Avenue de Général Leclerc, 35042 Rennes, France.
[c] J.J
Max-Planck-Institut für Chemishe Energiekonversion
Stiftstr. 34-36, D-45470,Mülheim an der Ruhr
Germany

Supporting information for this article is given via a link at the end of the document.

one NOPy ligand. The oxygen atom of the NOPy ligand bridges two $Dy(tta)_3$ as an inversion center is located in between the two Dy^{III} ions to afford a centro-symmetric dinuclear compound (Figure 1). The coordination environment of the Dy^{III} ion is a slightly distorted triangular dodecahedron (D_{2d} site symmetry, CSM=0.403)[66] while **DyPyNO** was made of slightly distorted square-antiprisms (Table S1, Figure 2). Dy-Oxygen bond lengths range between 2.30(6) Å and 2.43(1) Å and Dy-Dy distance is 4.15(6) Å (selected bond distances and angles are listed in Table S2). Two CH_2Cl_2 crystallization molecules lie in between the dimers. Each dimer is well isolated and the shortest inter-dimer Dy-Dy distance is 11.59(5) Å.

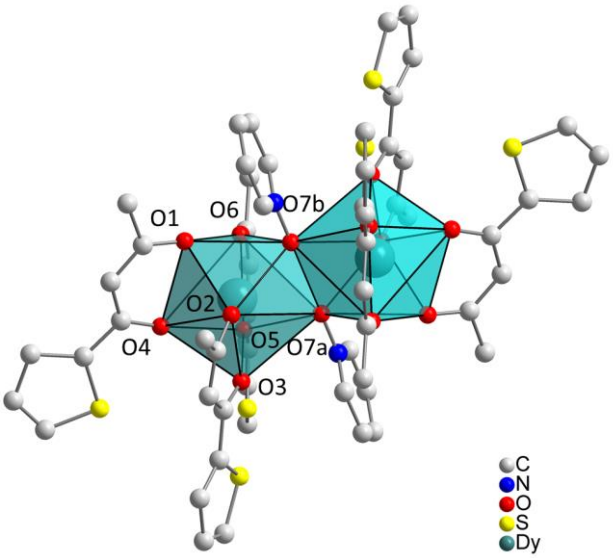

Figure 1. Representation of **Dy**, with coordination polyhedrons and atom labelling. Hydrogens and solvent atoms are omitted for clarity.

Easy magnetization axes calculated through *ab-initio* on **Dy** and **DyPyNO** are provided in Figure 2 and very similar features can be observed. On both compounds highly anisotropic Dy^{III} ions, with almost pure 15/2 ground state are found (g_z=19.58 and g_z =19.53 respectively, in the frame of the effective spin ½, Tables S11-S12). The ground states are well separated from the first excited states (160 cm^{-1} and 121 cm^{-1}, respectively). The substitution of the ancillary ligand does not have any significant influence on the orientation of the easy-magnetic axes (Figure 2), that despite the different symmetry of the coordination environment, are oriented almost strictly perpendicular to the Dy-Dy direction (calculated angles are 88.46° an 89.96° for **Dy** and **DyPyNO** respectively). This agrees with what is found on similar compounds where easy-magnetic axis orientation is not guided by coordination polyhedron symmetry but by global electrostatic considerations in the molecule.[14,15,18,21]

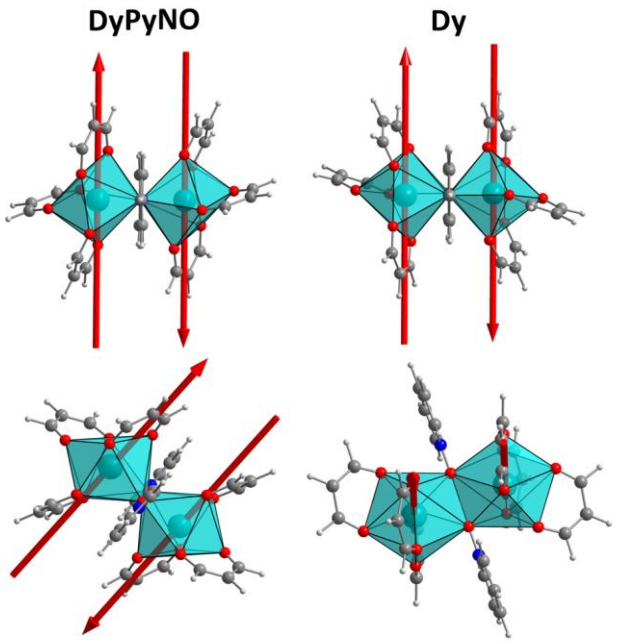

Figure 2. Representation of the molecular fragments of **DyPyNO** (left) and **Dy** (right) as considered for ab-initio calculations with calculated orientation of magnetic axes. Views are oriented perpendicular to the Dy-Dy direction (top) and as the best coordination polyhedron view (bottom) that are a triangular dodecahedron for **Dy** and a square antiprism for **DyPyNO**.

Magnetic measurements

Direct-current (dc) magnetic susceptibility studies were carried out on the three samples in the 2-300 K temperature range with a static field of 1 kOe (Figure S2). At room temperature, the $\chi_M T$ values are 27.76, 27.50 and 27.33 cm^3 K mol^{-1} for **161Dy**, **Dy** and **164Dy** respectively, *i.e.* close to the expected value for the free-ion (14.17 cm^3 K mol^{-1} for one Dy). On cooling, $\chi_M T$ products are essentially temperature independent in the 300-100K temperature range. On lowering the temperature a slow decrease is observed. These thermal behaviors are mostly due to progressive depopulation of excited M_J states of anisotropic Dy^{III} ions and weak antiferromagnetic interactions as observed on **DyPyNO**. This behavior is reproduced by *ab-initio* calculations taking into account an antiferromagnetic coupling of J_{total}=-2.86 cm^{-1}, in the frame of the effective spin ½.This value is obtained considering both dipolar J_{dip} and exchange J_{exch} contributions. J_{dip} =- 2.36 cm^{-1} is calculated on the basis of the Dy-Dy distance and of the relative angles between the easy magnetic axes as previously reported.[54] J_{exch}= -0.50 cm^{-1} is estimated by using the POLY_ANISO program (see computational details in SI).[67,68] Similar procedure on **DyPyNO** affords J_{total}= J_{dip} + J_{exch}= -2.44 -0.25 = -2.69 cm^{-1}. AF coupling seems so to be slightly weaker on **DyPyNO** than **Dy** as also observed experimentally (J_{exp}=-2.46 cm^{-1}).[55] This enhanced AF coupling on **Dy** is likely to be the reason why the SMM behavior is enhanced on this compound (see below).

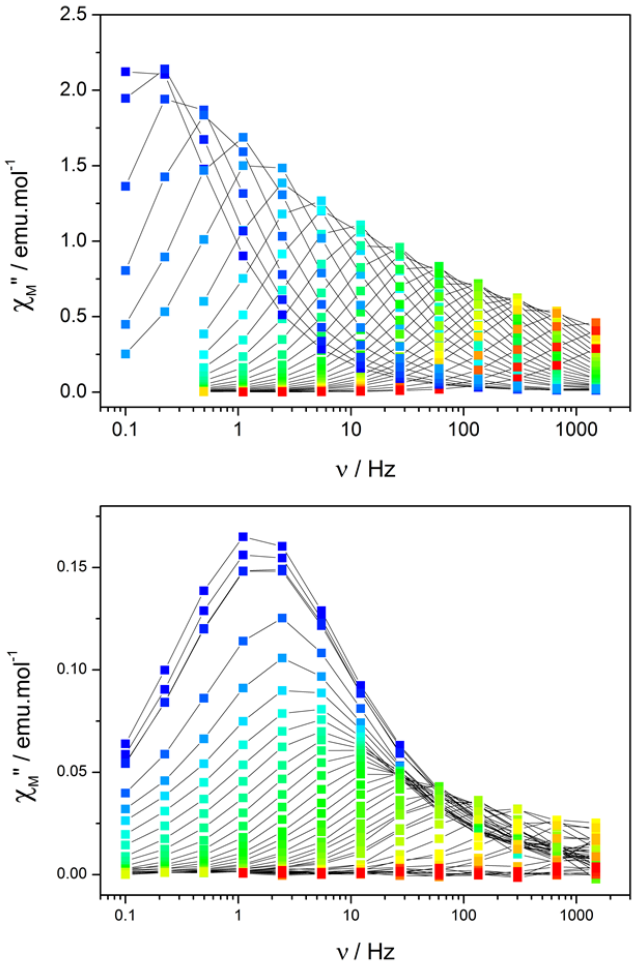

Figure 3. (Top) Frequency dependence of the *out-of*-phase component of the magnetization (χ_M'') of **Dy** in zero static magnetic field. (Bottom) Frequency dependence of the *out-of*-phase component of the magnetization (χ_M'') of **YDy** in zero static magnetic field. Color mapping from 1.8K (blue) to 20K (red). (0.1K spacing below 2K; 0.5K above). Lines are guides to the eye.

Dynamic magnetic behaviors have been investigated from 1.8 to 20 K in the 0.1-1500 Hz frequency range in the absence of an external field. Strong frequency dependence of the in-phase (χ_M') and out-of-phase (χ_M") components of the magnetization is observed on all derivatives (Figures S3-S15). As observed on the Arrhenius plot (Figure 4), the investigated temperature range corresponds to an intermediate between purely thermally activated and purely thermally independent behavior and uncertainty on the determination of dynamic parameters is quite high (τ_{2K}≈1.5s, Δ> 90 K) (Tables S3-S8). However, all derivatives have a clearly enhanced dynamic behavior compared to **DyPyNO** (τ_0= 5.62 10^{-11}s, Δ= 167 K). This is in agreement with *ab-initio* calculations that evidence an optimized separation between the ground state and the first excited state (160 cm^{-1} for **Dy** and 121 cm^{-1} for **DyPyNO**). Consequently the substitution of the ancillary ligands has a positive impact on the magnetic properties of the dimers. Last, the distribution of the relaxation times is small and indicates a homogenous SMM behavior (α_{10K-2K} = 0.05-0.20, 0.08-0.21 and 0.04-0.20 for **161Dy**, **Dy** and **164Dy** respectively) (Figure 5 and SI). All derivatives show a very large fraction of relaxing molecules with χ_M'/χ_T values for low frequencies close to zero (χ_T is the isotherm susceptibility).

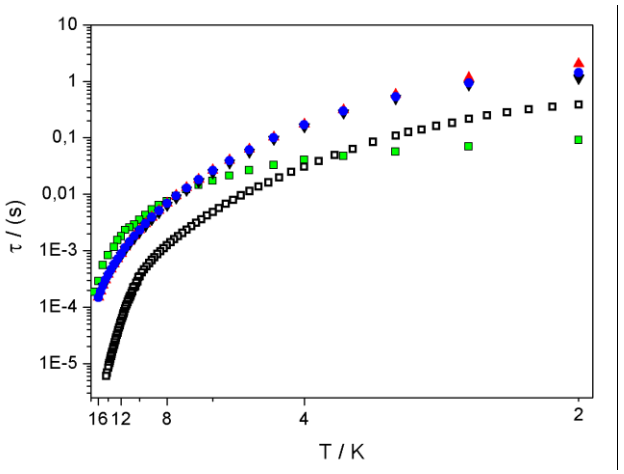

Figure 4. Arrhenius plot for **161Dy** (blue dots), **Dy** (black triangles), **164Dy** (red triangles) and **YDy** (green squares). **DyPyNO** (empty black squares) is added for comparison.

Contrary to what observed in our previous study on the isotopically-substituted mononuclear Dy-SMM[64] all dynamic features of the magnetic relaxation of **161Dy**, **Dy** and **164Dy** are highly similar. To have further insight on that point low temperature hysteresis measurements have been performed (Figures 6-7). Compared to **DyPyNO**, clear optimization of the SMM behavior is observed in line with the dynamic measurements. Hysteresis curves show the characteristic features of antiferromagnetically coupled dimers[25,55] with a stepped magnetization curve in zero-field followed by a successive closing of the hysteresis at low field. This particular field induces an acceleration of the magnetic relaxation because it corresponds to the level crossing between the first excited state and the ground state of the dimer. In the Ising approximation (S=1/2, g=g_z) this value is related to the coupling constant through $H_{crossing}$=-*J*/(2g_zβ).[55] Here $H_{crossing}$≈ 1600 Oe and provide J=-2.99 cm^{-1} (with a theoretical g_z=20) and J_{exp}=-2.92 cm^{-1} (with a calculated g_z=19.58, see ab-initio section). This is in agreement with what found by *ab-initio* calculations and with the trend in the value of $H_{crossing}$ when comparing **Dy** and **DyPyNO** hysteresis curves (Figure 6).

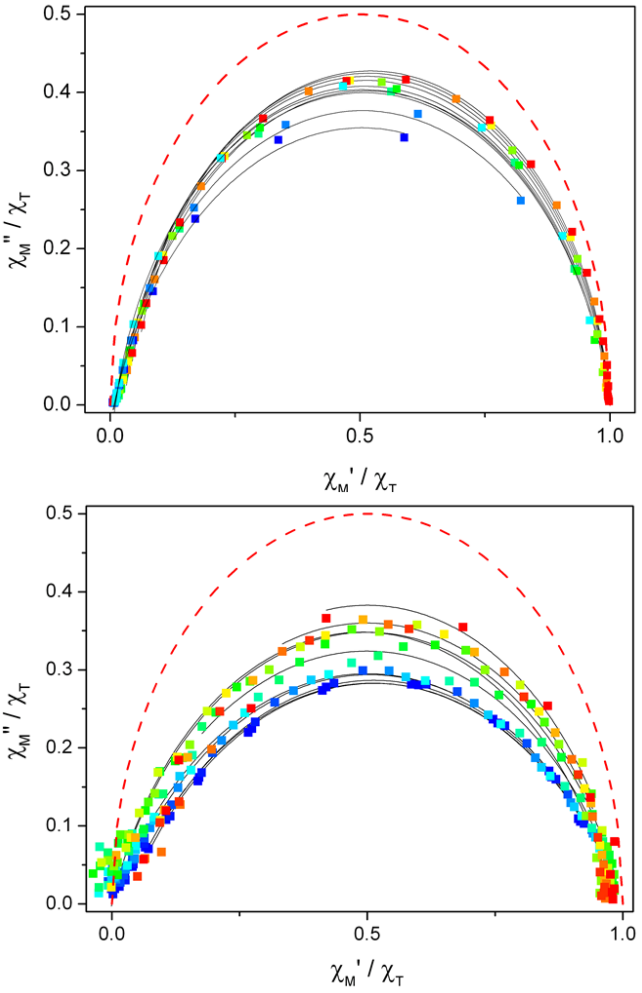

Figure 5. (Top) Normalized Argand plot for selected temperature between 3-11 K temperature range for **Dy.** (Bottom) Normalized Argand plot for selected temperature between 1.8-10 K for **YDy**. Lines represent the best fits as calculated with an extended Debye model. The dashed red line represents simulated curves for single relaxation process (α=0).

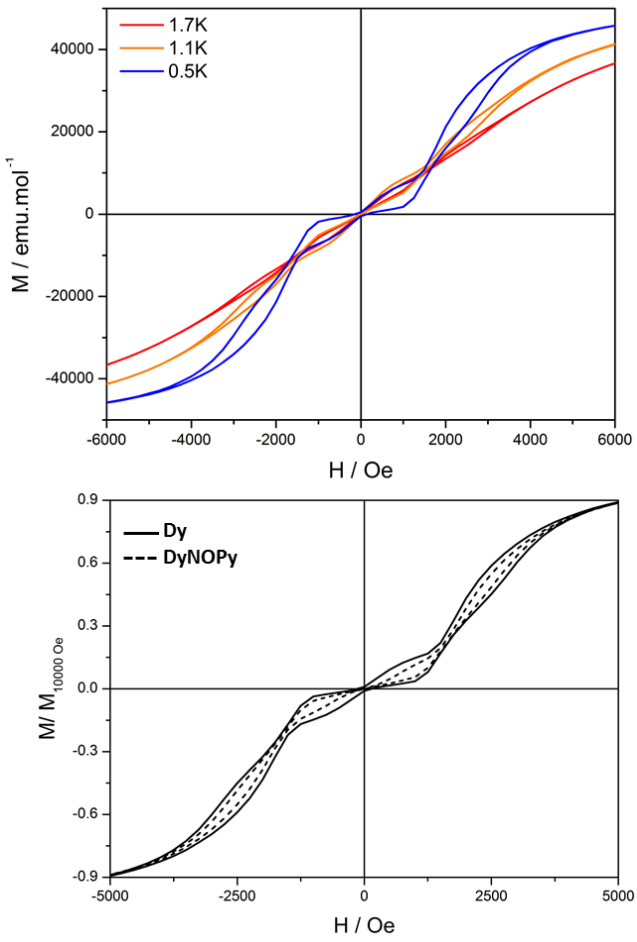

Figure 6. (Top) Hysteresis curves measured on **Dy** for various temperatures. (Bottom) Comparison of the hysteresis curves of **Dy** (full line) and **DyPyNO** (dotted line) at 0.5K (16 Oe.s^{-1} field sweep rate).

Isotopic substitution is expected to induce a closing (^{161}Dy, I=5/2, in **161Dy**) or an opening (^{164}Dy, I=0, in **164Dy**) of the hysteresis curves as the hyperfine interaction between Dy^{III} centers is enhanced or cancelled, respectively.[64] In first approximation, **Dy** is made of half I=5/2 and half I=0 species and is thus expected to show an averaged behavior. Here, this expected trend is weakly seen and only for the rising field hysteresis branch (absolute value). This significates that the benefit of isotopic substitution is overcame by all other competing interactions in the compounds such as dipolar or exchange interactions. This is also visible on dynamic magnetic measurements (Figure 4).

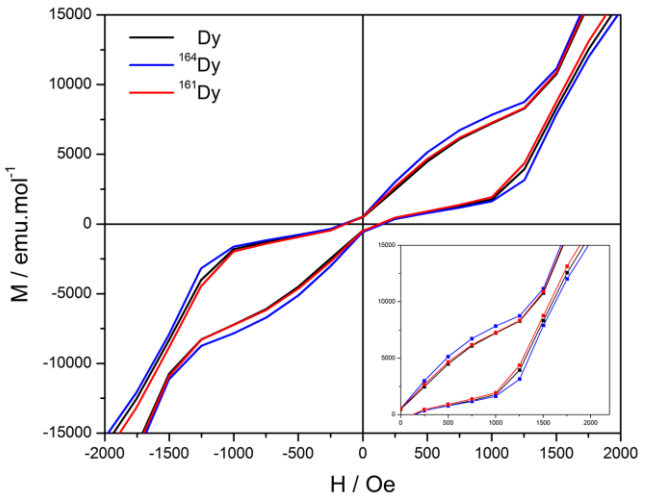

Figure 7. Comparison of the hysteresis curve of **161Dy** (red), **Dy** (black) and **164Dy** (blue) at 0.5K (16 Oe.s^{-1} field sweep rate).

We recently demonstrated that doping of the isotopically pure SMM into an amorphous diamagnetic matrix allows to significantly enhance the effect of isotopic substitution.[64] We have thus tested if diamagnetic dilution of the dimers is possible. To do so, two different samples have been synthesized. The first one is obtained by reacting a mixture of $Dy(hfac)_3{\cdot}2H_2O$ and $Y(hfac)_3{\cdot}2H_2O$ precursors in a 0.17/0.83 ratio with the NOPy ligand. The second one is obtained by dissolving $[Dy(tta)_3(NOPy)]_2$ and $[Y(tta)_3(NOPy)]_2$ dimers in the same 0.17/0.83 ratio and is latter called **YDy.** The resulting magnetic measurements of the two samples are totally similar. This sustains the hypothesis of a thermodynamically favored Y-Dy dimer over the pure homo-metallic Dy-Dy or Y-Y species during the recrystallization process. This is in line with previous studies on 4f-4f' compounds[69-73] and is a severe shortcoming for dilution experiments on such poly-nuclear species. The magnetic measurements of $[Dy_{0.17}Y_{0.83}(tta)_3(NOPy)]_2$ (**YDy**) shows that almost all the **YDy** sample is made of Y-Dy dimers as peaks related to **Dy** are not visible in ac measurement (figure 3) and Argand plots are remarkably clean from **Dy** contribution (figure 5).

Overall, dynamic magnetic behavior of **YDy** is drastically different from the one of **Dy** (Figures 3-5, S16-S20, Tables S9-S10). At high temperature the magnetic relaxation regime is very similar but a clear acceleration of the relaxation rate is observed at low temperature. Additionally, the distribution of the relaxation times is higher than in **Dy** and is indicative of several competing relaxing pathways ($\alpha_{10K\text{-}2K}$ = 0.17-0.32, Figure 5). This confirms that the intramolecular Dy-Dy antiferromagnetic interaction has a positive impact on the SMM properties of **Dy** and diminishes the occurrence of temperature independent relaxation pathways at low temperature. It is worth noting that we have drawn the same conclusion on a closely related but ferromagnetically coupled Dy-dimer.[54]

Conclusion

In conclusion, we report here an optimization of the SMM behavior of a Dy-based dimer by substitution of the ancillary ligands from hfac$^-$ to tta$^-$. The de-symmetrization of the ancillary ligand induces a deformation of the charge distribution around the Dy^{III} ion and provides a more favorable electrostatic environment for its magnetic slow relaxation. It also enhanced Dy-Dy antiferromagnetic coupling.

Isotopic substitution on the dimers has a very weak effect on the hysteresis curves, probably because of the strong antiferromagnetic interaction observed within the dimers. Additionally, we demonstrate that diamagnetic dilution of such polynuclear species only affords hetero-metallic Y-Dy dimers in which zero-field SMM behavior is dramatically damaged because of the suppression of the Dy-Dy AF interaction.

The design of magnetically coupled polynuclear Dy-based SMM molecules is then a possible way to weaken the temperature independent relaxation processes in zero-field that is usually observed on such SMMs.

Experimental Section

Synthesis: Pyridine N-oxide and 2-thenoyltrifluoroacetonate have been purchased from Aldrich chemicals, and used without further purification. Isotopically enriched dysprosium oxides (Dy_2O_3) have been purchased from Eurisotop. $^{161}Dy_2O_3$ is enriched at 92.2% in ^{161}Dy and $^{164}Dy_2O_3$ is enriched at 96.8% in ^{164}Dy. Corresponding $Dy(tta)_3{\cdot}2H_2O$ precursors have been synthesized according to the reported procedure.[64] **161Dy**, **164Dy** and **Dy** have been synthesized using the corresponding $Dy(tta)_3{\cdot}2H_2O$ precursor: 0.1 mmol of $Dy(tta)_3{\cdot}2H_2O$ is dissolved in 10 ml $CHCl_3$ and reacted with a Pyridine N-oxide solution (0.1 mmol in 10 ml $CHCl_3$) added drop-by-drop. The resulting solution is covered with a n-heptane layer and let for some days at 2°C. Pale yellow crystals are obtained after several days. Similar procedure has been used to synthesize **YDy** (see main text).

Crystal-structure determination: A single-crystal of **Dy** has been mounted on a APEXII AXS-Bruker diffractometer equipped with a CCD camera and a graphite-monochromated Mo-K_α radiation source (λ =0.71073 Å), from the Centre de Diffractométrie (CDiFX), Université de Rennes 1, France. Data were collected at 150K. Structure was solved with a direct method using the SIR-97 program[74] and refined with a full-matrix least-squares method on F^2 using the SHELXL program[75] and WinGX interface.[76] Structure was solved with a direct method using the SIR-97 program[74] and refined with a full-matrix least-squares method on F^2 using the SHELXL program[75] and WinGX interface.[76] Crystallographic data are summarized in Table 1. CCDC 1561799 contains the supplementary crystallographic data for this paper. These data can be obtained free of charge from The Cambridge Crystallographic Data Centre via www.ccdc.cam.ac.uk/data_request/cif.

Table 1. Main crystallographic information for **Dy**

Formula	$C_{59}\ H_{34}\ Dy_2\ Cl_2\ F_{18}\ N_2\ O_{14}\ S_6$
M [g.mol^{-1}]	1925.20
Crystal system	triclinic
Space group	P-1 (N°2)
a[Å]	12.273(5)
b[Å]	12.356(5)

c[Å]	13.891(5)
α[°]	114.102(5)
β[°]	109.086(5)
γ [°]	93.313(5)
V[Å^3]	1743.2(12)
Z	1
T[K]	150(2)
Θ max	27.500
Reflns collected	7907
Independant reflns	6748
Parameters	436
R1/wR2	0.0498/0.1589
Goof	0.975

X-ray powder diffraction: X-ray powder diffractograms were collected by a Panalytical X'pert Pro diffractometer equipped with an X'celerator detector. Recording conditions were 45 kV and 40 mA with Cu-K_α (λ=1.54 Å), in θ- θ mode in 5 min between 5° and 75° (8378 measurements). The calculated patterns were produced using the Mercury 3.0 software.

Magnetic measurements: Measurements were performed on a Quantum design MPMS magnetometer on polycrystalline samples compacted in pellets in order to avoid crystallite orientation under magnetic field. Measurements were corrected from the diamagnetic contributions calculated with Pascal constants. Hysteresis curves were measured with a ^{3}He insert in the same magnetometer with a field sweep rate of 16 Oe.s^{-1}

Ab-initio calculations: Wavefunction based calculations were carried out on **Dy** and **DyPyNO** by using the SA-CASSCF/RASSI-SO approach, as implemented in the MOLCAS quantum chemistry package (versions 8.0).[77] Further details can be found in supplementary materials.

Acknowledgements

We acknowledge financial support from CNRS, Université de Rennes 1, Region Bretagne, INSA Rennes, FEDER, Agence Nationale de la Recherche (ANR-13-BS07-0022-01), Rennes Metropole and China Scholarship Council. T Roisnel and V. Dorcet are acknowledged for their assistance in crystal structure data collection. B.L.G. thanks the French GENCI/IDRIS-CINES centre for high-performance computing resources.

Keywords: lanthanides • single-molecule magnets • isotope •magnetic properties •dysprosium

(1) D. Gatteschi; R. Sessoli; J. Villain *Molecular Nanomagnets*; Oxford University Press: Oxford, 2006.
(2) O. Kahn *Molecular Magnetism*; Wiley-VCH: Weinheim, 1993.
(3) Y.-C. Chen; J.-L. Liu; L. Ungur; J. Liu; Q.-W. Li; L.-F. Wang; Z.-P. Ni; L. F. Chibotaru; X.-M. Chen; M.-L. Tong; *J. Am. Chem. Soc.* **2016**, 2829-2837.
(4) J. D. Rinehart; M. Fang; W. J. Evans; J. R. Long; *Nat. Chem.* **2011**, *3*, 538-542.
(5) J. M. Zadrozny; D. J. Xiao; M. Atanasov; G. J. Long; F. Grandjean; F. Neese; J. R. Long; *Nat. Chem.* **2013**, *5*, 577-581.
(6) L. Ungur; J. J. Le Roy; I. Korobkov; M. Murugesu; L. F. Chibotaru; *Angew. Chem.-Int. Ed.* **2014**, *53*, 4413-4417.
(7) D. N. Woodruff; R. E. P. Winpenny; R. A. Layfield; *Chem. Rev.* **2013**, *113*, 5110-5148.
(8) J. Tang; P. Zhang In *Lanthanides and Actinides in Molecular Magnetism*; Wiley-VCH Verlag GmbH & Co. KGaA: 2015, p 61-88.
(9) J. Xiong; H.-Y. Ding; Y.-S. Meng; C. Gao; X.-J. Zhang; Z.-S. Meng; Y.-Q. Zhang; W. Shi; B.-W. Wang; S. Gao; *Chem. Sci.* **2017**, *8*, 1288-1294.
(10) R. Layfield; F.-S. Guo; B. Day; Y.-C. Chen; M.-L. Tong; A. Mansikamäkki; *Angew. Chem.-Int. Ed.* **2017**, ASAP.
(11) C. Benelli; D. Gatteschi *Introduction to Molecular Magnetism: From Transition Metals to Lanthanides*; Wiley, 2015.
(12) S. Gao *Molecular nanomagnets and related phenomena*; Springer, 2015; Vol. 164.
(13) In *Lanthanides and Actinides in Molecular Magnetism*; Wiley-VCH Verlag GmbH & Co. KGaA: 2015.
(14) J. Jung; X. Yi; G. Huang; G. Calvez; C. Daiguebonne; O. Guillou; O. Cador; A. Caneschi; T. Roisnel; B. Le Guennic; K. Bernot; *Dalton Trans.* **2015**, *44*, 18270-18275.
(15) J. Jung; F. Le Natur; O. Cador; F. Pointillart; G. Calvez; C. Daiguebonne; O. Guillou; T. Guizouarn; B. Le Guennic; K. Bernot; *Chem. Commun.* **2014**, *50*, 13346-13348.
(16) W.-B. Sun; P.-F. Yan; S.-D. Jiang; B.-W. Wang; Y.-Q. Zhang; H.-F. Li; P. Chen; Z.-M. Wang; S. Gao; *Chem. Sci.* **2016**, 684-691.
(17) S.-D. Jiang; S.-X. Qin; *Inorg. Chem. Front.* **2015**, *2*, 613-619.
(18) N. F. Chilton; D. Collison; E. J. L. McInnes; R. E. P. Winpenny; A. Soncini; *Nat. Commun.* **2013**, *4*, 2551.
(19) M. Gregson; N. F. Chilton; A.-M. Ariciu; F. Tuna; I. Crowe; W. Lewis; A. J. Blake; D. Collison; E. J. L. McInnes; R. E. P. Winpenny; S. Liddle; *Chem. Sci.* **2015**, 6655-6669.
(20) E. Moreno Pineda; N. F. Chilton; R. Marx; M. Dörfel; D. O. Sells; P. Neugebauer; S.-D. Jiang; D. Collison; J. van Slageren; E. J. L. McInnes; R. E. P. Winpenny; *Nat. Commun.* **2014**, *5*, 5243.
(21) N. F. Chilton; S. K. Langley; B. Moubaraki; A. Soncini; S. R. Batten; K. S. Murray; *Chem. Sci.* **2013**, *4*, 1719-1730.
(22) J. Liu; Y.-C. Chen; J.-L. Liu; V. Vieru; L. Ungur; J.-H. Jia; L. F. Chibotaru; Y. Lan; W. Wernsdorfer; S. Gao; X.-M. Chen; M.-L. Tong; *J. Am. Chem. Soc.* **2016**.
(23) M. Gysler; F. El Hallak; L. Ungur; R. Marx; M. Hakl; P. Neugebauer; Y. Rechkemmer; Y. Lan; I. Sheikin; M. Orlita; C. Anson; A K. Powell; R. Sessoli; L. Chibotaru; J. van Slageren; *Chem. Sci.* **2016**, 4347-4354.
(24) S. Xue; Y.-N. Guo; L. Ungur; J. Tang; L. F. Chibotaru; *Chem. Eur. J.* **2015**, *21*, 14099-14106.
(25) C. Y. Chow; H. Bolvin; V. E. Campbell; R. Guillot; J. W. Kampf; W. Wernsdorfer; F. Gendron; J. Autschbach; V. L. Pecoraro; T. Mallah; *Chem. Sci.* **2015**, *6*, 4148-4159.
(26) J. Jung; O. Cador; K. Bernot; F. Pointillart; J. Luzon; B. Le Guennic; *Beilstein J. Nanotechnol.* **2014**, *5*, 2267-2274.
(27) G. Cucinotta; M. Perfetti; J. Luzon; M. Etienne; P.-E. Car; A. Caneschi; G. Calvez; K. Bernot; R. Sessoli; *Angew. Chem.-Int. Edit.* **2012**, *51*, 1606-1610.
(28) M. Feng; S. Speed; F. Pointillart; B. Lefeuvre; B. Le Guennic; S. Golhen; O. Cador; L. Ouahab; *Eur. J. Inorg. Chem.* **2015**, *2016*, 2039-2050.
(29) J. D. Rinehart; J. R. Long; *Chem. Sci.* **2011**, *2*, 2078-2085.
(30) A. J. Brown; D. Pinkowicz; M. R. Saber; K. R. Dunbar; *Angew. Chem.-Int. Ed.* **2015**, 5864-5868.
(31) E. Lucaccini; L. Sorace; M. Perfetti; J. P. Costes; R. Sessoli; *Chem. Commun.* **2014**, *50*, 1648-1651.
(32) D. Aravena; E. Ruiz; *Inorg. Chem.* **2013**, *52*, 13770-13778.
(33) Y. Peng; V. Mereacre; A. Baniodeh; Y. Lan; M. Schlageter; G. E. Kostakis; A. K. Powell; *Inorg. Chem.* **2015**, 68-74.
(34) Y. Zhang; M. Bhadbhade; N. Scales; I. Karatchevtseva; J. R. Price; K. Lu; G. R. Lumpkin; *J. Solid State Chem.* **2014**, *219*, 1-8.
(35) W.-H. Zhu; S. Li; C. Gao; X. Xiong; Y. Zhang; L. Liu; A. K. Powell; S. Gao; *Dalton Trans.* **2016**, *45*, 4614-4621.

(36) W.-Y. Zhang; Y.-M. Tian; H.-F. Li; P. Chen; W.-B. Sun; Y.-Q. Zhang; P.-F. Yan; *Dalton Trans.* **2016**, *45*, 3863-3873.
(37) W. Yu; F. Schramm; E. M. Pineda; Y. Lan; O. Fuhr; J. Chen; H. Isshiki; W. Wernsdorfer; W. Wulfhekel; M. Ruben; *Beilstein J. Nanotechnol.* **2016**, *7*, 126-137.
(38) W. Sun; B. Yan; L. Jia; B.-W. Wang; Q. Yang; X. Cheng; H. Li; P. Chen; Z. Wang; S. Gao; *Dalton Trans.* **2016**, *45*, 8790-8794.
(39) L. F. Marques; A. Cuin; G. S. G. de Carvalho; M. V. dos Santos; S. J. L. Ribeiro; F. C. Machado; *Inorg. Chim. Acta* **2016**, *441*, 67-77.
(40) W.-M. Wang; H.-X. Zhang; S.-Y. Wang; H.-Y. Shen; H.-L. Gao; J.-Z. Cui; B. Zhao; *Inorg. Chem.* **2015**, *54*, 10610-10622.
(41) S.-Y. Lin; J. Wu; C. Wang; L. Zhao; J. Tang; *Eur. J. Inorg. Chem.* **2015**, *2015*, 5488-5494.
(42) H.-Y. Shen; W.-M. Wang; Y.-X. Bi; H.-L. Gao; S. Liu; J.-Z. Cui; *Dalton Trans.* **2015**, *44*, 18893-18901.
(43) F. Pointillart; S. Speed; B. Lefeuvre; F. Riobé; S. Golhen; B. Le Guennic; O. Cador; O. Maury; L. Ouahab; *Inorganics* **2015**, *3*, 554-572.
(44) C. Gao; A. M. Kirillov; W. Dou; X. Tang; L. Liu; X. Yan; Y. Xie; P. Zang; W. Liu; Y. Tang; *Inorg. Chem.* **2014**, *53*, 935-942.
(45) K. Suzuki; R. Sato; N. Mizuno; *Chem. Sci.* **2013**, *4*, 596-600.
(46) J.-D. Leng; J.-L. Liu; Y.-Z. Zheng; L. Ungur; L. F. Chibotaru; F.-S. Guo; M.-L. Tong; *Chem. Commun.* **2013**, *49*, 158-160.
(47) F. Habib; M. Murugesu; *Chem. Soc. Rev.* **2013**, *42*, 3278-3288.
(48) G. Cosquer; F. Pointillart; B. Le Guennic; Y. Le Gal; S. Golhen; O. Cador; L. Ouahab; *Inorg. Chem.* **2012**, *51*, 8488-8501.
(49) F. Pointillart; Y. Le Gal; S. Golhen; O. Cador; L. Ouahab; *Chem. Eur. J.* **2011**, *17*, 10397-10404.
(50) J. Long; F. Habib; P. H. Lin; I. Korobkov; G. Enright; L. Ungur; W. Wernsdorfer; L. F. Chibotaru; M. Murugesu; *J. Am. Chem. Soc.* **2011**, *133*, 5319-5328.
(51) D. Aguila; L. A. Barrios; F. Luis; A. Repolles; O. Roubeau; S. J. Teat; G. Aromi; *Inorg. Chem.* **2010**, *49*, 6784-6786.
(52) P. H. Lin; T. J. Burchell; R. Clerac; M. Murugesu; *Angew. Chem.-Int. Edit.* **2008**, *47*, 8848-8851.
(53) Y. Li; F. K. Zheng; X. Liu; W. Q. Zou; G. C. Guo; C. Z. Lu; J. S. Huang; *Inorg. Chem.* **2006**, *45*, 6308-6316.
(54) X. Yi; K. Bernot; O. Cador; J. Luzon; G. Calvez; C. Daiguebonne; O. Guillou; *Dalton Trans.* **2013**, *42*, 6728-6731.
(55) X. Yi; K. Bernot; F. Pointillart; G. Poneti; G. Calvez; C. Daiguebonne; O. Guillou; R. Sessoli; *Chem.-Eur. J.* **2012**, *18*, 11379-11387.
(56) L. Zhang ; J. Jung; P. Zhang; M. Guo; L. Zhao; J. Tang; B. Le Guennic; *Chem. Eur. J.* **2016**, *22*, 1392-1398.
(57) W.-M. Wang; W.-Z. Qiao; H.-X. Zhang; S.-Y. Wang; Y.-Y. Nie; H.-M. Chen; Z. Liu; H.-L. Gao; J.-Z. Cui; B. Zhao; *Dalton Trans.* **2016**, *45*, 8182-8191.
(58) Y.-L. Wang; C.-B. Han; Y.-Q. Zhang; Q.-Y. Liu; C.-M. Liu; S.-G. Yin; *Inorg. Chem.* **2016**, *55*, 5578-5584.
(59) F. Habib; G. Brunet; V. Vieru; I. Korobkov; L. F. Chibotaru; M. Murugesu; *J. Am. Chem. Soc.* **2013**, *135*, 13242-13245.
(60) L. Zhang; Y.-Q. Zhang; P. Zhang; L. Zhao; M. Guo; J. Tang; *Inorg. Chem.* **2017**.
(61) P. Comba; M. Großhauser; R. Klingeler; C. Koo; Y. Lan; D. Müller; J. Park; A. Powell; M. J. Riley; H. Wadepohl; *Inorg. Chem.* **2015**, *54*, 11247-11258.
(62) E. Kiefl; M. Mannini; K. Bernot; X. Yi; A. Amato; T. Leviant; A. Magnani; T. Prokscha; A. Suter; R. Sessoli; Z. Salman; *ACS Nano* **2016**, *10*, 5663-5669.
(63) I. Cimatti; X. Yi; R. Sessoli; B. Le Guennic; J. Jung; T. Guizouarn; A. Magnani; K. Bernot; M. Mannini; *Appl. Surf. Sci.* **2017**, in press.
(64) F. Pointillart; K. Bernot; S. Golhen; B. Le Guennic; T. Guizouarn; L. Ouahab; O. Cador; *Angew. Chem.-Int. Ed.* **2015**, *54*, 1504-1507.
(65) Y. Kishi; F. Pointillart; B. Lefeuvre; F. Riobe; B. Le Guennic; S. Golhen; O. Cador; O. Maury; H. Fujiwara; L. Ouahab; *Chem. Commun.* **2017**, *53*, 3575-3578.
(66) S. Alvarez; D. Avnir; M. Llunell; M. Pinsky; *New J. Chem.* **2002**, *26*, 996-1009.
(67) L. F. Chibotaru; L. Ungur; A. Soncini; *Angew. Chem.-Int. Edit.* **2008**, *47*, 4126-4129.
(68) L. F. Chibotaru; L. Ungur; C. Aronica; H. Elmoll; G. Pilet; D. Luneau; *J. Am. Chem. Soc.* **2008**, *130*, 12445-12455.
(69) T. Riis-Johannessen; N. Dalla Favera; T. K. Todorova; S. M. Huber; L. Gagliardi; C. Piguet; *Chem. Eur. J.* **2009**, *15*, 12702-12718.
(70) L. S. Natrajan; A. J. L. Villaraza; A. M. Kenwright; S. Faulkner; *Chem. Commun.* **2009**, 6020-6022.
(71) N. Dalla-Favera; J. Hamacek; M. Borkovec; D. Jeannerat; G. Ercolani; C. Piguet; *Inorg. Chem.* **2007**, *46*, 9312-9322.
(72) S. Floquet; M. Borkovec; G. Bernardinelli; A. Pinto; L.-A. Leuthold; G. Hopfgartner; D. Imbert; J.-C. G. Bünzli; C. Piguet; *Chem. Eur. J.* **2004**, *10*, 1091-1105.
(73) J. Gónzalez-Fabra; N. A. G. Bandeira; V. Velasco; L. A. Barrios; D. Aguilà; S. J. Teat; O. Roubeau; C. Bo; G. Aromí; *Chem. Eur. J.* **2017** *23*, 5117-5125.
(74) A. Altomare; M. C. Burla; M. Camalli; G. L. Cascarano; C. Giacovazzo; A. Guagliardi; A. G. G. Moliterni; G. Polidori; R. Spagna; *J. Appl. Crystallogr.* **1999**, *32*, 115-119.
(75) G. M. Sheldrick; *Acta Crystallogr. Sect. A* **2008**, *64*, 112-122.
(76) L. J. Farrugia; *J. Appl. Crystallogr.* **2012**, *45*, 849-854.
(77) F. Aquilante; L. De Vico; N. Ferre; G. Ghigo; P. Å. Malmqvist; P. Neogrady; T. B. Pedersen; M. Pitonak; M. Reiher; B. O. Roos; L. Serrano-Andres; M. Urban; V. Veryazov; R. Lindh; *J. Comput. Chem.* **2010**, *31*, 224-247.

10.1002/ejic.201700842

FULL PAPER

SMM optimization by ancillary ligand substitution on Dy-dimer is presented. Diamagnetic substitution highlights the positive impact of strong intermolecular AF interaction in dimers' SMM properties. This interaction is further responsible for the weak isotopic effect observed on the isotopically pure derivatives.

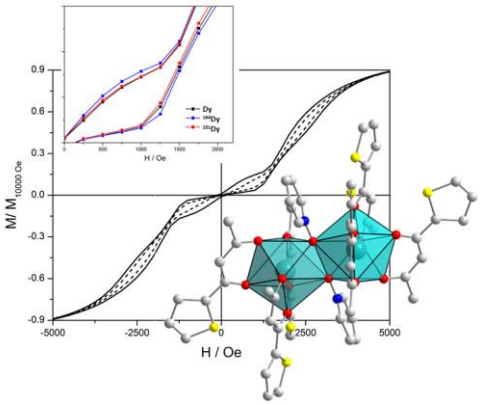

Lanthanide-based SMM*

*Xiaohui Yi, Gang Huang, Julie Jung, Olivier Guillou, Olivier Cador, Fabrice Pointillart, Boris Le Guennic and Kevin Bernot**

Page No. – Page No.

Optimization of magnetic relaxation and isotopic enrichment in dimeric Dy^{III} single-molecule magnets